1

2

3

4 **The C-terminus of the TlpD cytoplasmic chemoreceptor promotes polar localization and function**

5 *Running title: TlpD of* H. pylori *requires the C-terminal 45 amino acids*

6 Raymondo Lopez-Magaña[1] & Karen M. Ottemann[1,*]

7

8

9 [1]Department of Microbiology and Environmental Toxicology, UC Santa Cruz, Santa Cruz, CA

10

11 * Corresponding author

12 Email: Ottemann@ucsc.edu

Abstract

Bacteria localize proteins to distinct subcellular locations. One family of proteins with distinct cellular placement are chemoreceptors, which frequently localize to the bacterial pole. Although some polarity-promoting mechanisms have been described, there are many chemoreceptors that lack clear routes to becoming polar. The TlpD chemoreceptor of *Helicobacter pylori* is one such protein. *H. pylori* is a chemotactic bacterial pathogen with four chemoreceptors. Its cytoplasmic chemoreceptor, TlpD, localizes to the pole in a manner that is independent of the other chemoreceptors. In this work, we evaluated the role of TlpD domains in its function. Truncated proteins were created that lacked different amounts of the N- or C-termini and expressed in *H. pylori* in place of native *tlpD* or as the sole chemoreceptor. These TlpD variants were examined for expression, protein localization, association with chemotaxis signaling proteins, and effect on motility. TlpD that lacked any portion of the N-terminal 104 amino acids did not produce detectable protein. In contrast, TlpD retained expression with loss of the C-terminal 45 amino acids. TlpD variants lacking the last 45 amino acids (TlpDΔC4) preserved the ability to interact with CheW and CheV proteins based on bacterial two-hybrid analysis but were unable to localize to the pole either on their own or in the presence of other chemoreceptors. TlpDΔC4 was found diffuse in the cytoplasm, and recruited detectable CheV1, CheV2, and CheV3 to this location but not CheW. TlpDΔC4 did not confer chemotactic abilities. These findings suggest the C-terminal end of TlpD plays a previously unappreciated role in promoting TlpD polar localization. The mechanism by which TlpD drives polar localization could translate to soluble cytoplasmic chemoreceptors in other bacterial pathogens.

Author Summary

Although bacteria are small, they still place their proteins in specific locations that are required for the proteins to function. One such place is the bacterial end, or pole, where numerous proteins head to. How the bacterial cell identifies which proteins go to the pole is not fully understood. In this work, we dissect parts of a protein called TlpD that naturally goes to the pole. We find that mutants lacking one

end of TlpD lose their polar placement. TlpD is part of *H. pylori's* chemotaxis system, an ability that allows the bacteria to direct their motility towards beneficial situations and away from harmful ones. This ability is critical for infection in *H. pylori* and numerous other pathogens. When TlpD loses its polar placement, the protein no longer functions, laying the foundation for future studies that can translate into therapies to treat or prevent *H. pylori* infection.

Introduction

H. pylori is a human pathogen that infects approximately one-half of the world's population [1]. This bacterium infects the stomach and causes chronic stomach inflammation and gastric cancer [1]. To reach the stomach, *H. pylori* must navigate a dynamic environment. In route, *H. pylori* encounters various signals, including mammalian produced ones such as acid from stomach parietal cells and reactive oxygen from epithelial and innate immune cells [2–5]. One strategy *H. pylori* uses to circumvent these compounds, and find beneficial ones, is directed motility, also known as chemotaxis [6]. The chemotaxis signal transduction system, extensively studied in *Escherichia coli*, allows bacteria to sense concentration gradients of particular chemicals and initiate a motility response [7–10]. This chemotaxis system is required for *H. pylori* to establish infection [2,11–14]. The ability to sense and mount an appropriate response towards these signals allows effective navigation and infection.

The *H. pylori* chemotaxis system, like the *E. coli* one, operates as a multiprotein complex. Like that of well-studied bacteria, this complex forms via protein-protein interactions, including between sensors known as chemoreceptors, coupling proteins, and the CheA histidine kinase they control [15–17]. In contrast to the one-coupling protein system of *E. coli* that uses the canonical coupler CheW, the chemotaxis system of *H. pylori* contains three additional coupling proteins called CheV1, CheV2, and CheV3 [15,18]. These CheV paralogs are proposed to function in several ways, including as coupling proteins, phosphate sinks, or possibly as unique coupling proteins to accommodate chemoreceptors that

60 cannot couple to CheW [15,19,20]. In the *H. pylori* system, both CheW and CheV1 are critical to build
61 chemoreceptor arrays [16,17] and each CheV plays specific roles in motility [18,21]. However, the exact
62 roles of CheV2 and CheV3 in *H. pylori* chemotaxis have yet to be determined [15,16].

63 The *H. pylori* chemotaxis system uses four chemoreceptors called TlpA, TlpB, TlpC, and TlpD.
64 TlpA, TlpB and TlpC are integral membrane proteins whereas TlpD is cytoplasmic [6,22]. Soluble
65 cytoplasmic chemoreceptors like TlpD of *H. pylori* are uniquely positioned within the cell and not
66 membrane bound. This cytoplasmic chemoreceptor contains a C-terminal chemoreceptor zinc binding
67 (CZB) sensing domain [17,23]. Despite being cytoplasmic, TlpD localizes to the pole and retains this
68 capability even in the absence of any membrane bound chemoreceptors [17]. However, the mechanism
69 by which TlpD locates to the cell pole remains unclear.

70 TlpD also recruits other chemotaxis proteins to the cell pole. This chemoreceptor is sufficient to
71 recruit CheA, CheW, CheV1, and CheV3 proteins to the *H. pylori* cell pole [17]. TlpD likely interacts with
72 the CheW and CheV coupling proteins via its methyl accepting (MA) domain, as has been shown in other
73 chemoreceptors. Altogether, these properties of TlpD highlight this soluble cytoplasmic chemoreceptor
74 as a key component of the *H. pylori* chemotaxis system.

75 TlpD alone can form a functional signaling unit with core chemotaxis proteins. This
76 chemoreceptor interacts directly with coupling proteins CheW and CheV1 [16]. This interaction with
77 coupling proteins facilitates an indirect interaction with the CheA kinase to form a functional signaling
78 unit. Indeed, a combination of reconstituted TlpD, CheA and CheW or CheV1 proteins are sufficient to
79 drive CheA phosphorylation and suggest both can create a functional signaling unit in vitro [16] [24].
80 Moreover, *H. pylori* with TlpD as its only chemoreceptor retains spreading motility and further supports
81 a model by which TlpD alone forms an autonomous and functional signaling unit [17].

In this study, we created TlpD truncations and analyzed how these affect function in situ, expressing the proteins in the native *H. pylori*. Most truncations resulted in loss of stability in *H. pylori* but not *E. coli*. One mutant construct, however, was stably expressed in *H. pylori*: a C-terminus deletion of amino acids 388-433. This region is C-terminal to the CZB domain and based on bioinformatic analysis, had no detectable features or domains. This truncated protein, called TlpDΔC4, maintained its ability to interact with CheW and CheV coupling proteins, based on immunolocalization assays, but lost its ability to localize to the pole and function.

Results

The cytoplasmic chemoreceptor TlpD has only two identifiable domains: a central MA domain and a C-terminal CZB domain

Although previous work had identified domains of TlpD [23,24], we wanted to have up-to-date information about the protein, and therefore carried out bioinformatic analysis and identified end points of predicted domains. Toward that end, we used AlphaFold2 [25] to predict domains and structure of the 433 amino acid TlpD protein (Fig 1A). This approach identified, as expected, the previously known MA and CZB domains [23]. The MA domain spans amino acids 152 to 287 and sits proximal to the CZB domain, which spans from 315 to 379 (Fig 1B). Following the C-terminal CZB domain is a 54 amino acid stretch with no annotated domain (Figs 1A and 1B). The N-terminus comprises the first 140 amino acids and is predicted to orient perpendicular to the rest of the protein (Figs 1A and 1B). Like the C-terminus, the N-terminal stretch had no annotated motifs (Fig 1A). We then carried out further analysis to double check whether there were any potential domains at either terminus testing these individual sequences alone or in the full-length protein using multiple bioinformatic servers including MotifFinder, NCBI CDD, Protein CCD, [26–28]. These servers, however, identified no domains (S1 Fig and S1 File). Secondary

105 structure analysis using Globplot [29] determined TlpD was entirely structured except for two regions,
106 151 to 160 and 351 to 358, that lack any secondary structure (S1 Fig). Protein-protein interactions may
107 structure these disorganized regions [29,30]. Indeed, regions 151 to 160 are located inside the MA
108 domain, and 351 to 358 sit inside the CZB domain, and are likely to be structured based on
109 crystallography of other CZB proteins [31]. Overall, these analyses suggest that TlpD has known domains
110 in the middle portion, while the N- and C-termini are predicted to be folded into a secondary structures
111 but any lack identifiable domains.

112 Because it is unclear what the functions of the TlpD N- or C-terminus are, we took advantage of
113 the two-domain architecture of TlpD to create truncated versions that removed select regions but
114 retained the MA or CZB domains. Truncation constructs of TlpD were designed to omit portions of the N
115 or C-termini (Fig 1B). An initial round of constructs did not avoid predicted secondary structure
116 endpoints, and resulted in proteins that were not expressed in *H. pylori* (S2 Fig). We hypothesized this
117 lack of expression could be due to interruption within secondary structures, so therefore redesigned the
118 truncations to avoid predicted secondary structure endpoints (S1 and S2 Files). We also included a
119 3xFLAG tag sequence at the C-terminus of some constructs to improve detectability. We designed these
120 constructs to integrate into the non-essential *rdxA* locus of *H. pylori*, facilitated by an erythromycin
121 resistance marker for positive selection and flanking *rdxA* sequences (S3A Fig). We also included 200bp
122 upstream of *tlpD* to capture potential promoters. This entire sequence was synthetically generated and
123 placed onto a high copy vector to allow manipulation in *E. coli* (Tables 1 and 2).

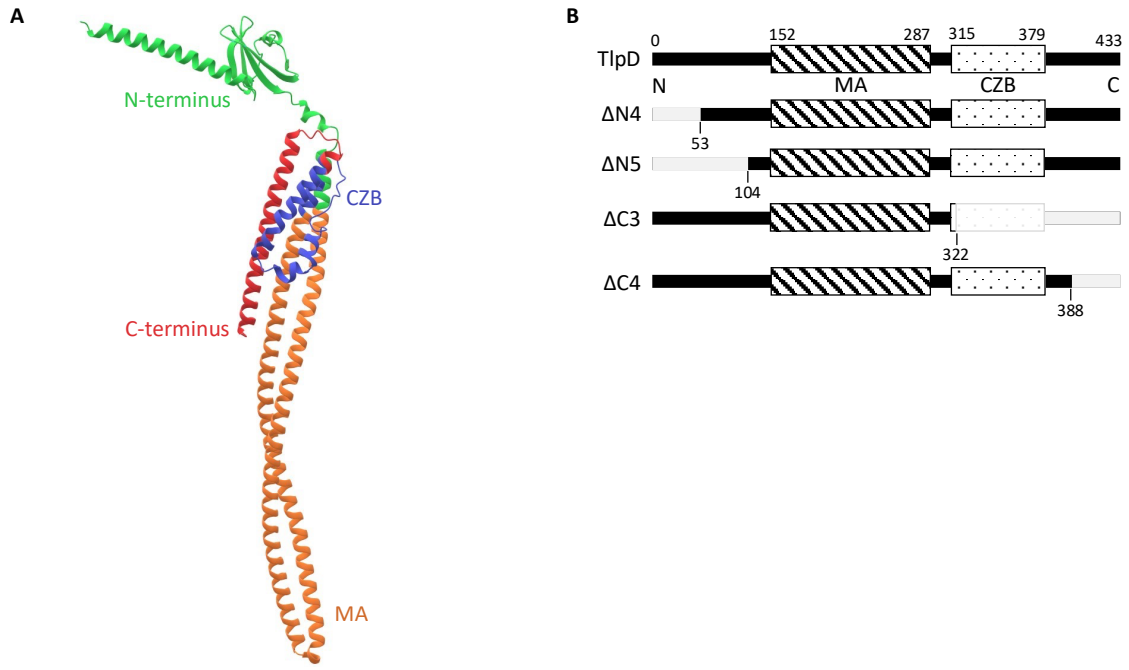

Fig 1. *H. pylori* TlpD predicted structure and domains. (A) AlphaFold predicted structure of *H. pylori* TlpD. TlpD is 433 amino acids in length with two known domains, the MA domain (orange) and CZB domain (blue). Regions with no known domains at the N-terminus are shown in green, and a C-terminal 54 amino acid stretch with no predicted domain is shown in red. (B) Diagram of modified versions of *H. pylori* TlpD with domains and truncation sites indicated (grey). TlpD is the full-length version of the protein at 433 amino acids, ΔN4 is truncated at residue 53, ΔN5 is truncated at residue 104, ΔC3 is truncated at residue 322, and ΔC4 is truncated at residue 388. Each of these constructs contains a C-terminal 3xFLAG tag.

Table 1. Plasmids used in this study.

Plasmid	KO reference no.	Genotype/description	Reference/source
DH10B pTwist *tlpD 3xflag*	KO1926	*rdxA::tlpD 3xflag erm*	This study
DH10B pTwist *tlpDΔN4*	KO1927	*rdxA::tlpDΔN4 3xflag erm*	This study
DH10B pTwist *tlpDΔN5*	KO1928	*rdxA::tlpDΔN5 3xflag erm*	This study
DH10B pTwist *tlpDΔC3*	KO1929	*rdxA::tlpDΔC3 3xflag erm*	This study

DH10B pTwist *tlpDΔC4*	KO1930	*rdxA::tlpDΔC4 3xflag erm*	This study
DH10B pTwist *tlpD*	KO1936	*rdxA::tlpD erm*	This study
pUT18	KO1346	BACTH vector	[32]; J. Gober, UCLA
pUT18C	KO1347	BACTH vector	[32]; J. Gober, UCLA
pKT25-zip	KO1348	BACTH pos. control vector	[32]; J. Gober, UCLA
pUT18C-zip	KO1349	BACTH neg. control vector	[32]; J. Gober, UCLA
XL1-Blue pUT18C-*tlpD*	KO1954	BACTH. G27 *tlpD* cloned on the C-terminus of pUT18C.	This study
XL1-Blue pUT18C-*tlpDΔC4*	KO1956	BACTH. G27 truncated *tlpDΔC4* cloned on the C-terminus of pUT18C.	This study
DH5a *cheV1*-pKNT25	KO1432	BACTH. G27 *cheV1* cloned on the N-terminus of pKNT25	(Abedrabbo et al., 2017)
DH5a *cheW*-pKTN25	KO1434	BACTH. G27 *cheW* cloned on the N-terminus of pKNT25	(Abedrabbo et al., 2017)

133

Table 2. Bacterial strains used in this study.

Strain	KO reference no.	Genotype/description	Reference/source
G27	KO379		[33], Nina Salama
G27 *ΔtlpD*	KO1165	*rdxA::kan-sac ΔtlpD::cat*	[34]
G27 *ΔtlpD, rdxA::tlpD 3xflag*	KO1931	KO1165 transformed with pTwist *tlpD 3xflag*	This study
G27 *ΔtlpD, rdxA::tlpDΔN4*	KO1932	KO1165 transformed with pTwist *tlpDΔN4*	This study
G27 *ΔtlpD, rdxA::tlpDΔN5*	KO1933	KO1165 transformed with pTwist *tlpDΔN5*	This study
G27 *ΔtlpD, rdxA::tlpDΔC3*	KO1934	KO1165 transformed with pTwist *tlpDΔC3*	This study

G27 *ΔtlpD, rdxA::tlpDΔC4*	KO1935	KO1165 transformed with pTwist *tlpDΔC4*	This study
*m*G27	KO625	Mouse adapted G27	[35]
mG27 ΔtlpD	KO1006	KO625 *ΔtlpD::cat*	[36]
*m*G27 *Δabcd*	KO1021	*ΔtlpA ΔtlpB ΔtlpC::aphA3 ΔtlpD::cat*	[17,37]
*m*G27 *Δabcd, rdxA::tlpD*	KO1940	KO1021 transformed with pTwist *tlpD*	This study
*m*G27 *Δabcd, rdxA::tlpDΔC4*	KO1941	KO1021 transformed with pTwist *tlpDΔC4 3xflag*	This study

TlpD lacking the 45 C-terminal amino acids is expressed in *H. pylori*

To evaluate the production of these TlpD constructs, we first evaluated protein expression from each plasmid in *E. coli* by western blot (Fig 2A). Full-length (TlpD) and versions of TlpD missing 53 (ΔN4) or 104 (ΔN5) amino acids of the N-terminus were detected at high levels (Fig 2A), suggesting the N-terminal regions are not required for expression in *E. coli*. Additionally, TlpD that omits the CZB domain (ΔC3), which is located at the C-terminal end but retains the MA domain and sequences N-terminal to it was also detected. However, TlpD missing 45 amino acids (ΔC4) of the C-terminus was minimally detectable in *E. coli*. Altogether, our ability to detect TlpD in *E. coli* gave us confidence that these truncations can produce stable protein.

We next wondered whether these constructs would produce protein in *H. pylori*. Each *tlpD* construct was transformed into *H. pylori* G27 *ΔtlpD* (Table 2), where they integrated the *tlpD*-portion into the genome at the *rdxA* locus, to confer erythromycin resistance (S3A Fig). Proper integration was confirmed by PCR using primers that flank the *rdxA* locus (S3B Fig). We then evaluated protein expression in *H. pylori* whole cell lysates by western blotting using an anti-FLAG antibody, as used in *E. coli* (Fig 2B). For this approach, *H. pylori* strains were grown on standard solid media (CHBA),

150 scraped from the plate, and diluted to an OD_{600} of 0.7 in PBS, and then whole cells collected by
151 centrifugation and lysed, to allow normalization based on OD_{600}. The Full-length TlpD (TlpD) was
152 detected when expressed from the *rdxA* locus (Fig 2B), but strains expressing N-terminus truncated
153 proteins (TlpD ΔN4 and ΔN5) had little or no protein detected (Fig 2B). Strains expressing C-terminus
154 truncated proteins (TlpD ΔC3 and ΔC4) varied in the amounts of protein detected: ΔC3 had a low signal,
155 similar to TlpDΔN5, while TlpDΔC4 had a clearly detectable signal that was approximately half that of WT
156 TlpD (Fig 2B). These findings suggest the C-terminal end of TlpD can be removed with minimal effect on
157 protein expression, in comparison to loss of any amount of the N-terminus or CZB domain which
158 resulted in very little protein detected. It was surprising that the various truncated TlpD proteins
159 expressed differentially between *E. coli* and *H. pylori*. However, because TlpD without the 45 C-terminal
160 amino acids was expressed to reasonable levels in *H. pylori*, we used this protein to characterize the role
161 of TlpD's C-terminal portion.

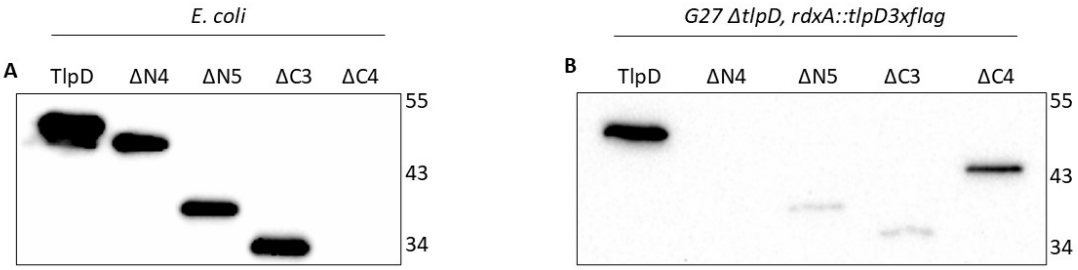

162

163 **Fig 2. TlpD FLAG-tagged truncations are produced in *E. coli* and *H. pylori ΔtlpD*.** (A) Western blot of *E.*
164 *coli* DH10B strains expressing TlpD from a plasmid were analyzed from whole-cell lysates with an anti-
165 FLAG antibody which recognizes the C-terminal tag. (B) Whole-cell lysates of *H. pylori* G27 Δ*tlpD* strains
166 complemented with *tlpD* constructs were similarly analyzed. The TlpD variant expressed is indicated at
167 the top, with TlpD indicating full length with the 3XFLAG. Marker sizes are given in kilodaltons on the
168 right. The expected size of TlpD is 51 kDa, ΔN4 is 45 kDa, ΔN5 is 39 kDa, ΔC3 is 38 kDa, and ΔC4 is 45 kDa.
169 Western blots are representative of 3 biological replicates.

170

171 **TlpDΔC4 does not confer soft agar migration in *H. pylori***

172 To begin our characterization of the TlpD C-terminal portion, we first analyzed the chemotaxis
173 ability of strains bearing this version of TlpD. We used a field-standard chemotaxis assay, migration in
174 soft agar. In this assay, bacteria are inoculated at a single point, and if motile and chemotactic, migrate
175 outwards to form expanded colonies. We initially analyzed G27 strains bearing the other
176 chemoreceptors, TlpA and TlpB, and found there was no difference ± *tlpD* or *tlpDΔC4* (S4 Fig). The soft
177 agar spreading of these isogenic *tlpD* complemented strains did not reach wild-type levels, and was not
178 different from the Δ*tlpD* parent (S4 Fig). We then analyzed strains that bear WT or truncated TlpD as
179 their only chemoreceptor. To this end, we complemented a strain of *H. pylori* that lacks all
180 chemoreceptors (mG27 *Δabcd*) with either a full-length TlpD or truncated TlpDΔC4. Of note, we were
181 only able to obtain strains for full length TlpD using the allele that lacked the FLAG tag; repeated
182 attempts to complement mG27 *Δabcd* with the 3xFLAG version of TlpD were unsuccessful. Expression of
183 the non-FLAG allele was confirmed using an anti-TlpA22 antibody (S5 Fig).

184 Next, the chemotaxis ability of these strains was measured by soft agar migration. Wild-type *H.*
185 *pylori* achieved the greatest spread diameter, while *H. pylori Δabcd* showed no spreading (Figs. 3A and
186 3C), as reported before [17]. Spreading of the strain with only full length TlpD complement (*rdxA::tlpD*)
187 was detectable by day three, with increased diameters that were significantly different from its
188 receptorless (*Δabcd*) counterpart, although below that of its wild type mG27 parent (Figs 3A and 3C).
189 These findings suggest that complementation of wild-type *tlpD* in the *rdxA* locus is partially sufficient to
190 restore spreading motility in *H. pylori*. Additionally, the spreading observed is attributed to the presence
191 of TlpD, as it is the only chemoreceptor present. The spreading motility of the TlpDΔC4 complemented
192 strain was similarly analyzed (Figs 3B and 3D). The TlpDΔC4 strain did not spread even after seven days

193 and phenocopied the *Δabcd* strain (Figs 3B and 3D). This finding suggests that truncation of the C-
194 terminus of TlpD results in a chemoreceptor that is insufficient to restore spreading. These findings
195 suggest that TlpDΔC4 may be unable to establish a working chemotaxis system.

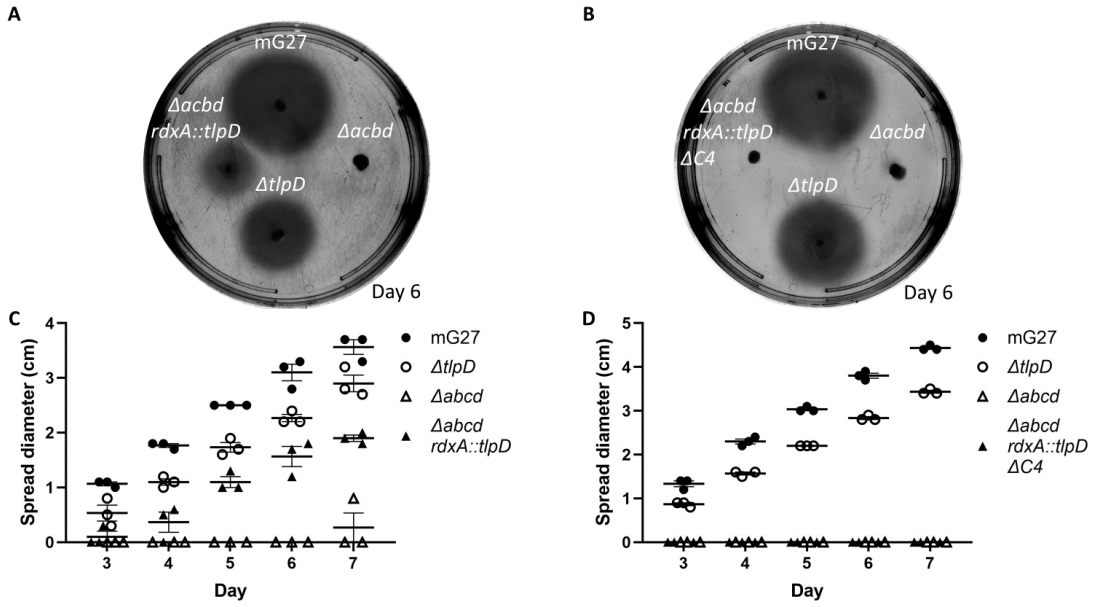

196

197 **Fig 3. *H. pylori* that express TlpDΔC4 as the sole chemoreceptor do not spread on soft agar.** (A) *H. pylori*
198 wild-type mG27 and isogenic mutants were analyzed for chemotaxis by soft agar spreading. Strains were
199 stabbed onto soft agar and spreading was tracked and measured after 3 days. Strains included are *H.*
200 *pylori* lacking all receptor (*Δabcd*), and isogenic versions complemented with a full-length TlpD
201 (*rdxA::tlpD*) (A-B) or with TlpDΔC4 (*rdxA::tlpD ΔC4*) (C-D). Graph includes 3 technical replicates and is
202 representative of 3 biological replicates, wild-type mG27 is a positive control and mG27 *Δabcd* is a
203 negative control. The error bars represent the standard error of the mean.

204

205 **TlpDΔC4 is unable to localize to the *H. pylori* cell pole**

206 TlpD normally localizes to the cell pole even when it is the only chemoreceptor present [17].
207 However, how exactly this chemoreceptor on its own establishes cell polarity is unknown. We wondered

208 how truncated TlpDΔC4 would localize within *H. pylori* that lacks all chemoreceptors. To this end, we
209 used immunofluorescence to investigate localization of the *H. pylori* receptorless strain (mG27 *Δabcd*)
210 complemented with either full-length TlpD or TlpDΔC4 (Table 2). Full-length TlpD localized to the pole
211 even when it is the only chemoreceptor present, as previously shown for a strain of *H. pylori* with
212 natively expressed TlpD [17] (Fig 4A). In contrast, TlpDΔC4 was diffuse and present throughout the
213 bacterium's cell cytoplasm (Fig 4A). These findings suggest that TlpD's C-terminal 45 amino acids are
214 important for polar localization.

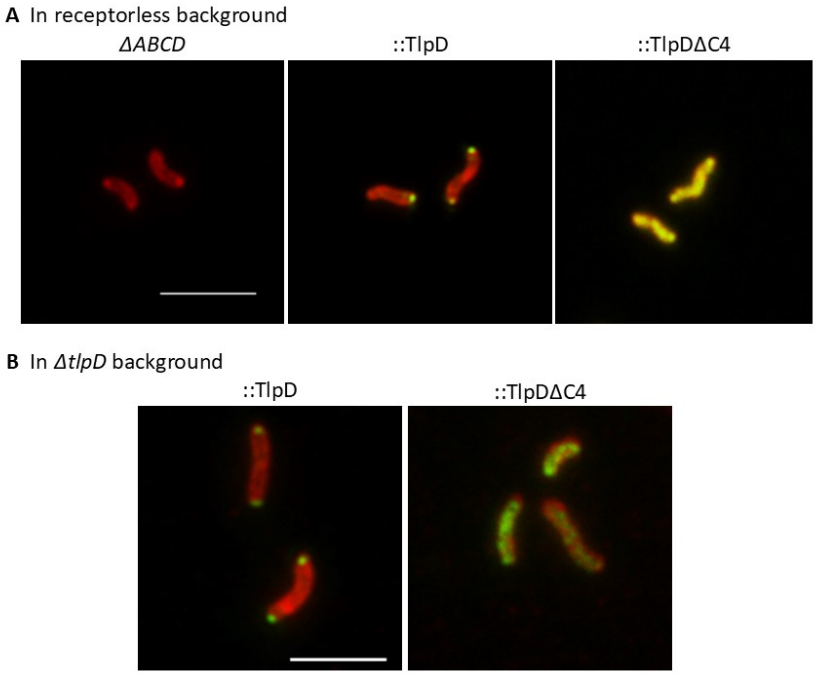

215

216 **Fig 4. TlpD is polar when the C-terminus is intact and diffused when the C-terminus is disrupted.**
217 Immunolocalization of *H. pylori* whole cells producing full-length or truncated TlpDΔC4 protein. *H. pylori*
218 was detected with chicken anti-*H. pylori* followed by goat anti-chicken conjugated to AlexaFluor 594
219 (red). TlpD proteins indicated above each image were detected with preabsorbed rabbit anti-TlpA22
220 (ΔABCD, TlpD) or rat anti-FLAG (TlpD, Δ4) followed by goat anti-rabbit or goat anti-rat conjugated to

221 AlexaFluor 488 (green). Scale bar = 4µM. Images are representative of 3 biological replicates, with 20-50
222 bacterial cells analyzed for each sample.

223

224 Because TlpD is one of four *H. pylori* chemoreceptors, we wondered how TlpDΔC4 would localize
225 when the other chemoreceptors were present. For this analysis, we made use of the FLAG tag to identify
226 TlpD specifically (Fig 4B). Full-length TlpD was found at the pole, as previously shown for a non-tagged
227 version of this protein [17] (Fig 4B). TlpDΔC4 was diffused, in contrast, and dispersed throughout the cell
228 cytoplasm (Fig 4B). These findings suggest that the TlpDΔC4 does not localize to the pole, even with
229 other chemoreceptors present. Additionally, these results suggest the C-terminal FLAG tag does not
230 impede full-length TlpD from polar localization. Altogether, using two different *H. pylori* strain
231 backgrounds, these findings further support the finding that the C-terminal portion of TlpD is important
232 for self-localization.

233 **Diffused TlpD disrupts localization of chemotaxis coupling proteins CheV1, CheV2, and CheV3**
234 **but not CheW**

235 The above results show that TlpDΔC4 does not localize to the pole as does full-length TlpD does,
236 even when the other chemoreceptors are present. We reasoned that TlpDΔC4 might either have lost the
237 ability to interact with the *H. pylori* coupling proteins or lost a region key for localization. To assess
238 whether TlpDΔC4 retained the ability to interact with the coupling proteins, we first asked how the
239 diffuse TlpDΔC4 would affect localization of these *H. pylori* chemotaxis signaling proteins in a background
240 that has TlpA and TlpB present. We used immunofluorescence of coupling proteins in *H. pylori* with
241 TlpDΔC4 (Fig 5). When full-length TlpD was present, all CheV and CheW proteins were entirely polar,
242 with no detectable cytoplasmic staining as previously shown [17] (Fig 5). In contrast, when TlpDΔC4 was
243 present, CheV1, CheV2, and CheV3 displayed both polar and nonpolar staining, with CheV3 showing the

244 most diffused cytoplasmic signal (Fig 5). CheW, in comparison, was entirely polar in the presence of

245 diffused TlpD. These results suggest that the diffused TlpDΔC4 retains the ability to interact with the

246 CheV proteins and can retain them in the cytoplasm.

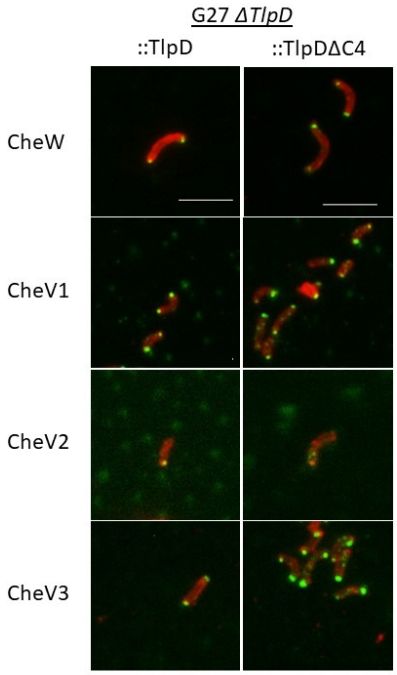

247

248 **Fig 5. Localization of CheW and CheV coupling proteins in the presence of TlpD-ΔC4.**

249 Immunolocalization of *H. pylori* chemotaxis proteins CheW, CheV1, CheV2, and CheV3 in whole cells

250 producing full-length (TlpD-FLAG) or truncated (TlpDΔC4-FLAG) protein. *H. pylori* was detected with

251 chicken anti-*H. pylori* followed by goat anti-chicken conjugated to AlexaFluor 594 (red). Individual

252 chemotaxis proteins indicated on the left were detected with preabsorbed guinea pig anti-CheW, rabbit

253 anti-CheV1, rabbit anti-CheV2 or rabbit anti-CheV3 followed by goat anti-guinea pig or goat anti-rabbit

254 conjugated to AlexaFluor 488 (green). Scale bar = 4μM. Images are representative of 3 biological

255 replicates, with 20-50 bacterial cells analyzed for each sample.

256

257 **C-terminus truncated TlpDΔC4 retains interaction with CheV1 and CheW in vitro**

258 Subcellular localization of chemotaxis proteins in *H. pylori* suggests TlpDΔC4 retains the ability to
259 interact with the CheV proteins (Fig 5). To further confirm that TlpDΔC4 retains the ability to interact
260 with the coupling proteins, we used bacterial two-hybrid (BACTH) analysis to examine interactions
261 between TlpDΔC4 and CheV1, as a model for CheV interactions, or CheW (Fig 6). We generated full-
262 length or truncated *tlpD* fused to the T18C fragment at the C- termini (T18C-*tlpD*, T18C-*tlpDΔC4*). These
263 plasmids were then co-transformed with NT25 fragment plasmids with *cheV1* (*cheV1*-NT25)
264 or *cheW* (*cheW*-NT25) used previously [16]. We found that full-length TlpD interacted with CheV1 to a
265 greater extent than CheW (Fig 6A and 6C), as previously shown [16]. Similarly, TlpDΔC4 interacted with
266 CheV1 and CheW (Fig 6B and 6C). The interactions of TlpDΔC4 were not seen by the colorimetric
267 indicator (Fig 6B) however measurement of β-gal activity shows a significant interaction with both CheV1
268 and CheW (Fig 6C). This result further supports that the truncated TlpDΔC4 retains binding function with
269 both CheV1 and CheW, suggesting the TlpD MA domain is correctly folded.

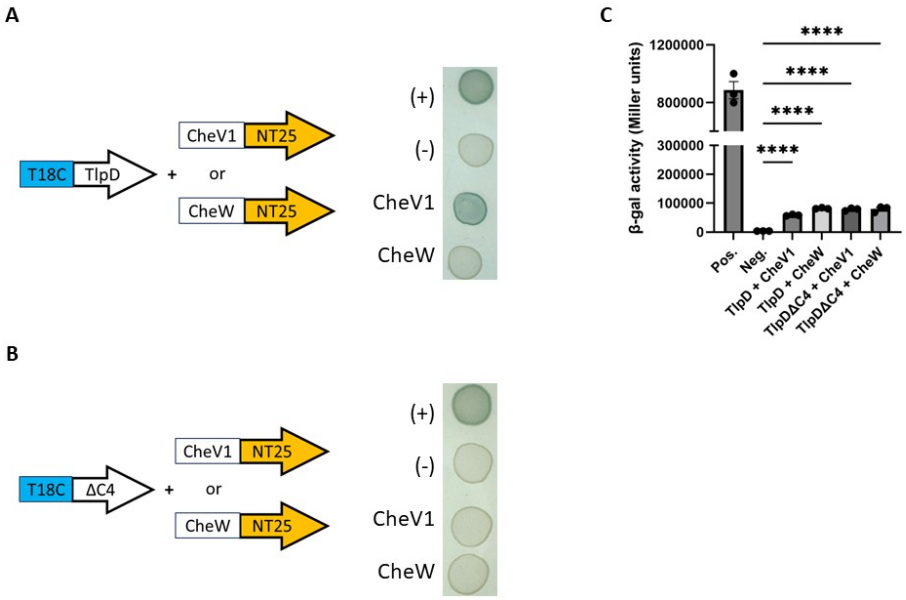

270

271 **Fig 6. TlpD's interaction with chemotaxis proteins is retained when the C-terminus is truncated.** BACTH

272 spot and β-galactosidase (β-gal) assays of (A)(B) full-length (TlpD) and (C)(D) truncated (TlpDΔC4) TlpD C-
273 termini of the T18C fragments and tested for interaction with CheV1 and CheW fused to the N-termini of
274 the T25 fragments in *E. coli* BTH101 cells. Liquid overnights were spotted onto LB containing X-gal, IPTG,
275 Amp, and Kan. Spot plates are representative of 3 biological replicates. Positive (+) controls are T25-zip
276 and T18-zip. Negative (-) controls are the respective TlpD construct with blank T25 plasmids. β-gal
277 activity of each interaction was measured, and Miller units were calculated to determine total activity. β-
278 gal activity is one biological replicate with three technical replicates per sample. Error bars indicate the
279 SEMs. Strains were analyzed statistically by an ordinary one-way ANOVA comparing the mean of each
280 column with the mean of the negative column. ****P<0.0001.

281

282 **Discussion**

283 Our experiments with a truncated version of the cytoplasmic protein TlpD revealed that TlpD
284 polar localization requires its C-terminal 45 amino acids. We reached this conclusion using
285 immunofluorescence of FLAG-tagged full length TlpD or FLAG-tagged TlpDΔC4. Full length TlpD-FLAG
286 localized to the pole as reported for TlpD lacking the FLAG [17], suggesting the FLAG tag did not disrupt
287 any localization signals. TlpDΔC4-FLAG, in contrast, did not display polar localization, suggesting that the
288 C-terminal 45 amino acids are critical for localization directly or for allowing TlpD to adopt a form that
289 can localize. Our analysis furthermore suggests that the TlpDΔC4 protein can at least partially fold, based
290 on its ability to maintain interactions with CheW and CheV proteins in *H. pylori* and CheV1 and CheW in
291 the BACTH assays. Interestingly, CheV proteins mislocalized to the cytoplasm more than CheW did when
292 TlpDΔC4 was present, suggesting that TlpD might have an interaction preference for CheV proteins
293 versus CheW, as suggested by previous BACTH studies of TlpD [16] and seen in *Campylobacter jejuni*

294 chemoreceptors [38]. Overall, these findings support the new idea that TlpD requires its C-terminal 45
295 amino acids to properly localize.

296 Given the importance of the C-terminal region, we checked carefully to see if there are any
297 motifs or features in it. Our search to identify features within the C-terminal 45 amino acids of TlpD,
298 however, revealed no apparent hits. This stretch of amino acids may contain a cryptic signal yet to be
299 identified. The AlphaFold structure described here suggests that this region adopts an extended 43
300 amino acid alpha helix that sits alongside the MA and CZB domains on one side, leaving the other side
301 exposed on the surface (Fig 1A). Thus, this region may play a structural or regulatory role, or possibly
302 interact with distinct proteins. TlpD's secondary structure analysis predicts that this protein is rigid,
303 similar to other chemoreceptors, and contains only two predicted flexible regions. The first flexible
304 region sits within the MA domain at residues 151-160, and the second sits inside the CZB domain at
305 residues 351-358. These flexible protein regions lack a predicted regular secondary structure, and
306 binding interactions could cause these regions to become ordered [29]. Future studies analyzing the TlpD
307 C-terminal stretch, and the disordered regions will be useful to provide further insight into the workings
308 of this cytoplasmic protein.

309 A potential function of this C-terminal stretch is in promoting protein-protein interactions that
310 either allow TlpD to reside at the pole or promote TlpD function. Two proteins, aconitase (AcnB) and
311 catalase (KatA) have been shown to interact with TlpD based on pull downs from *H. pylori* extracts [39].
312 Other proteins such as acetone carboxylase (HP0599) [40] and sialic acid binding protein (HP0721)
313 [41,42] are proposed to interact with TlpD based on two-hybrid assays. It is not yet known how these
314 proteins contribute to TlpD localization or function, an area important to follow up.

315 TlpD plays a critical role in building the chemotaxis protein arrays. Previous work had shown that
316 TlpD as the sole chemoreceptor localizes to the pole, and is sufficient to localize the main components of

317 the chemotaxis signaling complex—CheA, CheW, CheV1 and CheV3 to the cell pole too [17].
318 Furthermore, unpublished work with *H. pylori* that expressed only one transmembrane chemoreceptor,
319 either TlpA or TlpB, and lacked TlpD, mislocalized all three CheV proteins [43]. These studies suggest
320 TlpD plays a critical role in promoting chemotaxis proteins to localize to the pole. Our localization studies
321 showed that even when using an *H. pylori* strain that retained TlpA and TlpB, two transmembrane
322 chemoreceptors, the TlpDΔC4 was not at the pole and mislocalized CheV proteins. These findings
323 suggest that transmembrane chemoreceptors of *H. pylori* are not sufficient to maintain a distinctly polar
324 chemotaxis complex, but rather require polar TlpD.

325 These findings provide insight into the workings of cytoplasmic chemoreceptor proteins. The
326 cytoplasmic chemoreceptors that localize to the cell pole do so by colocalization with transmembrane
327 chemoreceptors [44–46], and in some cases switch between a diffused cytoplasmic protein and a distinct
328 polar topology [47]. Cytoplasmic chemoreceptors presumably utilize similar mechanisms used by other
329 chemoreceptors to drive polar localization including stochastic self-assembly, interaction with polar
330 anchor proteins, or interactions with plasmid partition homologues [48]. Our findings suggest that TlpD
331 may act as an anchor for chemotaxis coupling proteins to reach the pole as part of the chemotaxis
332 complex. TlpD contains a CZB domain, and our findings may be specific to these types of
333 chemoreceptors. One candidate for comparative analysis is the CZB-containing cytoplasmic
334 chemoreceptor McpA (NCBI Ref Seq: WP_000475246.1) from the enteric pathogen *Salmonella enterica*.
335 McpA is 352 amino acid protein and identified as an MA domain containing cytoplasmic chemoreceptor
336 with C-terminal CZB domain and an N-terminal coiled coil [49,50]. Later researchers found that *S.*
337 *enterica* that lacks seven of its nine chemoreceptors, and retains only McpA and another of unknown
338 function, Tip, fail to spread on soft agar [51,52]. McpA was not the focus of these previous studies,
339 however the findings do suggest this protein is not sufficient to confer a spreading phenotype in *S.*
340 *enterica*. No studies have focused on the role of McpA as a sensing protein or on its localization. Domain

341 architecture analysis of McpA shows a central MA domain, followed by a C-terminus coiled coil that
342 spans amino acids 314-344. This architecture is like that of TlpD however differs in the location of a
343 predicted coiled coil; C-terminal for McpA and N-terminal for TlpD [50]. Alignment of full length TlpD and
344 McpA shows 33% amino acid identity over the entire protein, and the C-terminal domains share 29%
345 amino acid identity. Moreover, McpA retains the conserved CZB motif (**H**xx[WFYL]x_{21-}
346 $_{28}$**C**x[LFMVI]Gx[WFLVI]x_{18-27}**H**xxx**H**) at its C-terminus (amino acids 246-303) [23]. The localization of McpA
347 is not yet known however and will be interesting for future studies.

348 In sum, our work supports that TlpD plays a central role in building a functional chemosensory
349 complex at the pole and relies on the sequences at its C-terminal end to accomplish this function. One
350 model, consistent with our data, is that the C-terminus of TlpD interacts with an as-yet-identified polar
351 landmark protein, to bring TlpD to the pole. Once there, TlpD plays a critical role in nucleating
352 chemosensory array formation. Testing this model and exploring whether other cytoplasmic
353 chemoreceptors have similar localization sequences is an exciting area for future work.

354 Materials and Methods

355 **Bacterial strains and growth conditions.** All *H. pylori* and *E. coli* strains used in this study are listed in
356 Tables 1 and 2. *H. pylori* was grown on Columbia Horse Blood Agar (CHBA) containing 5% (vol/vol)
357 defibrinated horse blood (Hemostat Labs, Davis, CA), 0.2% (wt/vol) β-cyclodextrin (TCI), 5 µg/mL
358 cefsulodin (Sigma Aldrich), 50 µg/mL cycloheximide (GoldBio), 2.5 U/mL polymyxin B (Sigma Aldrich) and
359 10 µg/mL vancomycin (GoldBio). For the selection of *H. pylori* mutants, 13 µg/mL chloramphenicol, 15
360 µg/mL kanamycin (Fisher BioReagents), or 25 µg/mL erythromycin (GoldBio) was used. For liquid
361 cultures, *H. pylori* was grown with brucella broth containing 10% heat-inactivated fetal bovine serum
362 (Gibco) (BB10). Cultures were incubated at 37°C in microaerobic conditions (5% O_2, 10% CO_2, and 85%

363 N_2). *E. coli* was grown on LB media containing 100 µg/mL ampicillin or 30 µg/mL kanamycin (Fisher
364 BioReagents) and incubated at 37°C unless otherwise stated.

365 **Strategy for creation of truncated TlpD.** To construct truncated versions of G27 TlpD (Uniprot:B5Z6X0),
366 Protein CCD [28] was used to identify predicted secondary structures, features, and domains within the
367 protein and served as the basis for selecting truncation sites that avoid secondary structures and
368 predicted or known regions. TlpD N-terminal truncations at amino acids 53 (ΔN4) and 104 (ΔN5), were
369 selected to sit in between secondary structures. The TlpD C-terminus truncations at amino acids 322
370 (ΔC3) and 388 (ΔC4) were selected to abolish or retain the CZB domain without interrupting the
371 canonical MA domain, respectively. Additionally, 200bp upstream of *tlpD* was included to capture any
372 transcriptional regulatory sites and sequences encoding a 3xFLAG tag (DYKDDDDK-DYKDDDDK-
373 DYKDDDDK) was added to the C-terminus of TlpD. Lastly, an erythromycin resistance gene and its
374 promoter were added for positive selection, downstream of *tlpD*. This entire sequence was flanked by
375 500bp upstream and downstream of the non-native locus, *rdxA*, for chromosomal integration in *H.*
376 *pylori*. pTwist Amp High Copy plasmids with ampicillin resistance were ordered from Twist Bioscience
377 that contained these *tlpD* cassette sequences (S2 File). These plasmids were then transformed into
378 electrocompetent *E. coli* DH10B cells using ampicillin selection followed by single colony purification.

379 **Creation of G27 and mG27 *tlpD* complement mutants.** For transformation into *H. pylori*, plasmids
380 containing *tlpD* sequences were purified from *E. coli* DH10B cells using the QIAprep Spin Miniprep Kit
381 (Qiagen) and added to a suspension of BB10 and 1-day old *H. pylori* G27 *ΔtlpD* or *ΔtlpA ΔtlpB ΔtlpC ΔtlpD*
382 cells from a CHBA plate [53]. Transformants were selected by growth on CHBA containing 25 µg/mL
383 erythromycin followed by single colony purification. All mutations were verified using PCR with primers
384 that flank *rdxA* (*rdxA* Fwd and Rev) (S3 Table).

385 **Western blot.** The expression of modified TlpD was observed by western blot. Liquid overnights of *E. coli*
386 were grown and used to prepare lysate samples. 1-to-2-day old *H. pylori* grown on CHBA solid media
387 containing erythromycin were resuspended in 1X Phosphate-Buffered Saline (PBS) and used to prepare
388 lysate samples. To prepare the lysate, samples were back diluted to OD_{600} = 0.7 in 200 µL. 6X SDS PAGE
389 sample buffer was added to the mixture at 1X final concentration and 1X PBS was added to 200 µL. Next,
390 samples were heated at 95-100°C for 10 minutes then placed on ice. Samples were electrophoresed on
391 10% or 12% SDS-PAGE gels then semi-dry transferred to polyvinylidene (PVDF) membranes using a trans-
392 blot SD semi-dry transfer cell (Bio-Rad). Relative protein loading was visualized by staining the
393 membrane with Direct Blue 71 (DB71) stain containing 0.008% DB71 (Sigma Aldrich) in 40% EtOH and
394 10% acetic acid prior to antibody binding. PVDF membranes were incubated with a 1:20,000 dilution of
395 rat anti-FLAG monoclonal antibody (Novus Biological, NBP1-06712) or a 1:4,000 to 1:10,000 dilution of
396 rabbit anti-TlpA22 antibody [34] diluted in 5% BSA at 4°C overnight. Membranes were next incubated
397 with a 1:20,000 dilution of horseradish peroxidase-conjugated goat anti-rat (R&D Systems) or a 1:10,000
398 dilution of goat anti-rabbit (Santa Cruz Biotechnology) secondary antibody. For visualization, SuperSignal
399 West Pico PLUS Chemiluminescent Substrate (Thermo Scientific) was added at a 1:1 ratio for 30 to 120
400 seconds with shaking at room temperature. Blots were then imaged using a Bio-rad Chemi-doc.

401 **Soft-agar motility assay.** *H. pylori* spreading motility was carried out as previously described [17,54–56].
402 Briefly, soft agar plates were made with brucella broth and 0.35% bacto agar (BD). Soft agar was cooled
403 to 50°C before 2.5% heat-inactivated fetal bovine serum, 8 µg/mL amphotericin B, 5 µg/mL cefsulodin,
404 50 µg/mL cycloheximide, 2.5 U/mL polymyxin B, 5 µg/mL trimethoprim (Sigma Aldrich), and 10 µg/mL
405 vancomycin were added. Plates set for 3 days at room temperature before use. 1–2-day old *H. pylori*
406 strains from CHBA plates were inoculated halfway into the agar using a pipet tip. Plates were incubated
407 right side up in the 37°C microaerobic chamber and migration diameter was measured daily. mG27,

408 mG27 *ΔtlpD*, and mG27 *ΔtlpA ΔtlpB ΔtlpC ΔtlpD* were used as controls. Statistical analysis was done on
409 GraphPad Prism v9.4.1.

410 **Immunofluorescence.** Immunolocalization of *H. pylori* chemotaxis proteins TlpD, CheW, CheV1, CheV2,
411 and CheV3 was performed as previously described [17,37]. Briefly, 1-day old *H. pylori* grown on Columbia
412 Horse Blood Agar (CHBA) under microaerobic conditions was harvested and resuspended in 1mL of 1X
413 PBS. 20 µL of the cell suspension was placed on a Poly-Lysine glass slide (Fisher Scientific) and fixed with
414 0.075M $NaPO_4$ adjusted to pH7.4, 0.0025M NaCl and 2% paraformaldehyde (EMS) solution then
415 permeabilized in 3% Bovine Serum Albumin (BSA) (Millipore), 1% Saponin (Calbiochem), 0.01% Triton X-
416 100 and 0.02% Na Azide (Sigma Aldrich) resuspended in 1X PBS. The samples were blocked with 3% BSA
417 and 0.01% Triton X-100 resuspended in 1X PBS solution. Samples were next treated with a 1:500 dilution
418 of chicken anti-*H.pylori* (Agrisera AB), a 1:2,000 dilution of rat anti-FLAG (Novus Biological, NBP1-06712),
419 a 1:200 of preabsorbed or non-preabsorbed rabbit anti-TlpA22, or a 1:50 dilution of preabsorbed rabbit
420 anti-CheV1 [37], anti-CheV2, anti-CheV3 (J. Castellon, P. Lertsethtakarn, and K.M. Ottemann,
421 unpublished), or guinea pig anti-CheW [17] diluted in permeabilization solution (described above). The
422 samples were then treated with a 1:500 dilution of goat anti-chicken Alexa Fluor 594 (Invitrogen,
423 A11042) and goat anti-rat Alexa Fluor 488 (ThermoFisher, A48262) or a 1:300 dilution of goat anti-rabbit
424 Alexa Fluor 488 (Invitrogen, A11008) or goat anti-guinea pig Alexa Fluor 488 (Invitrogen, A11073) diluted
425 in permeabilization solution. The samples were washed with blocking solution (described above) 3 times,
426 a drop of Vectashield (Vector Laboratories) was added to the cells and then sealed with coverslips.
427 Fluorescence microscopy, using the Nikon Eclipse E600 was used to visualize immunofluorescent cells at
428 100X objective with oil immersion. Texas Red and Fitc/GFP filters were used to separately view and
429 capture emission spectra from Alexa Fluor 594 (red) and 488 (green), respectively. Images were captured
430 using a Hamamatsu ORCA-285 digital camera equipped to the microscope. Fluorescent images were

431 pseudo colored using ImageJ and merged using Adobe Photoshop version 24.1.0. Scale = 4 µm. Images
432 are representative of 3 biological replicates.

433 **Creation of Bacterial Two-hybrid (BACTH) plasmids and BACTH analysis.** Synthetic plasmid DNA from *E.*
434 *coli* DH10B was extracted using the Qiaprep Mini Kit (Qiagen). *H. pylori* G27 full-length *tlpD* and
435 truncated *tlpDΔC4* constructs were amplified using PCR with primers that amplify each sequence (*tlpD*
436 pUT18 Fwd and Rev, *ΔC4* pUT18 Fwd and Rev) (S3 Table). The PCR products encoded PstI and SacI
437 restriction sites which were digested with Pst1-HF (NEB) and SacI-HF (NEB) restriction enzymes. BACTH
438 plasmids pUT18 and pUT18C (J. Gober, UCLA) [32] were similarly digested followed by phosphatase
439 treatment using rSAP following the manufacturer's suggested protocol (NEB). Treated PCR products and
440 plasmids were purified using the GFX PCR DNA and Gel Band Purification Kit (Cytiva). The purified
441 products were ligated using T4 DNA ligase following the manufacturer's suggested protocol (NEB) and
442 subcloned into electrocompetent *E. coli* XL1-Blue cells and ampicillin resistant colonies were selected. All
443 constructs were confirmed using PCR with the same primers used to amplify *tlpD* or *tlpDΔC4* (S3 Table)
444 and DNA sequencing (Azenta).

445 Recombinant plasmids encoding the *cheV1*-NT25 [16], *cheW*-T25 [16], T18C-*tlpD*, T18C-*tlpDΔC4* and
446 were co-transformed, at 40 ng each, into electrocompetent BTH101 and plated on LB containing 40
447 µg/mL X-gal (5-bromo-4-chloro-3-ondolyl-beta-galacto-pyranoside) (GoldBio), 0.5 mM IPTG (Isopropyl β-
448 d-1-thiogalactopyranoside) (Fisher BioReagents), 100 µg/mL ampicillin, and 50 µg/mL kanamycin. As
449 positive controls, T25-zip and T18-zip plasmids were co-transformed into BTH101. As negative controls,
450 each *tlpD* recombinant plasmid was co-transformed with a pKNT25 blank BACTH plasmids. For
451 interaction assays, colonies including controls grown on LB containing X-gal, IPTG, ampicillin, and
452 kanamycin at the above-mentioned concentrations were used to make overnights in LB with ampicillin
453 and kanamycin at the above concentrations. The following day, 20 µL of each overnight was dropped
454 onto LB plates containing X-gal, IPTG, ampicillin, and kanamycin as above. These spots were allowed to

455 dry at room temperature before the plates were incubated at 30°C for 24 hours. Images were captured
456 using an iPhone 14 Pro and a white light transilluminator (Fisher Scientific). Images are representative of
457 3 biological replicates.

458 **β-Galactosidase Assay.** To quantify BACTH interactions, β-galactosidase activity was measured as
459 previously described [16,32]. Briefly, transformants were grown in LB broth with ampicillin, kanamycin,
460 and IPTG at the above concentrations at 30°C overnight. Overnight cultures were back diluted to OD_{600}=
461 0.1 in LB broth with ampicillin, kanamycin, and IPTG then grown at 30°C until OD_{600} 0.3-0.7 was reached.
462 100 µL of each culture was mixed with 900 µL cold Z-Buffer (0.06M $Na_2HPO_4.7H_2O$, 0.04M $NaH_2PO_4.H_2O$,
463 0.01M KCl, 0.001M $MgSO_4.7H_2O$, adjusted to pH 7.0 and 0.05M β-mercaptoethanol was added fresh
464 before use) in triplicate and mixed by inversion. Next, 50 µL of 0.1% SDS and 100 µL of chloroform was
465 added to each sample followed by a 10 second vortex. The samples and fresh 4mg/mL ortho-
466 Nitrophenyl-β-galactoside (ONPG) (Thermo Scientific) (in 0.1M Phosphate Buffer solution (0.06M
467 $Na_2HPO_4.7H_2O$ and 0.04M $NaH_2PO_4.H_2O$ adjusted to pH 7.0) were incubated at 30°C for 5 minutes. 200
468 µL ONPG solution was added to samples, vortexed, and time was recorded. The samples were incubated
469 at 30°C until a yellow color appeared. The reactions were stopped by adding 500 µL Stop solution (1M
470 Na_2CO_3), time recorded, and samples centrifuged at max speed for 5 minutes before OD_{420} was
471 measured. Miller units were calculated to determine β-galactosidase activity using the following
472 formula: 1000 x (OD_{420} / [time * vol. culture * OD_{600}]) [57]. β-gal activity is one biological replicate with
473 three technical replicates per sample. Statistical analysis was done on GraphPad Prism v9.4.1.

474 **Acknowledgements**

475 We thank Fitnat Yildiz, Carrie Partch, and Chad Saltikov for discussion and support. We also thank UCSC
476 STEM Diversity for their support, particularly Yulianna Ortega and Xingci Situ. We are grateful to past and
477 current Ottemann lab members for their continued support throughout this project, particularly Arturo

Valdez and Christina Yang. The described project was supported by the National Institute of Allergy and Infectious Diseases (NIAID) grant RO1AI116946 to K.M.O. The funders had no role in study design, data collection, and interpretation, or decision to submit the work for publication.

481 **References**

482 1. Malfertheiner P, Camargo MC, El-Omar E, Liou JM, Peek R, Schulz C, et al. *Helicobacter pylori*
483 infection. Nat Rev Dis Prim. 2023;9(1).

484 2. Collins KD, Hu S, Grasberger H, Kao JY, Ottemann KM. Chemotaxis allows bacteria to overcome
485 host-generated reactive oxygen species that constrain gland colonization. Infect Immun
486 [Internet]. 2018;(March):IAI.00878-17.

487 3. Flint A, Stintzi A, Saraiva LM. Oxidative and nitrosative stress defences of *Helicobacter* and
488 *Campylobacter* species that counteract mammalian immunity. FEMS Microbiol Rev.
489 2016;40(6):938–60.

490 4. Grasberger, H., El-Zaatari, M. and Merchant J. Dual Oxidases Control Release of Hydrogen
491 Peroxide by the Gastric Epithelium to Prevent *Helicobacter felis* Infection and Inflammation in
492 Mice. Gastroenterology. 2013;145(5):1045–54.

493 5. Handa O, Naito Y, Yoshikawa T. *Helicobacter pylori:* A ROS-inducing bacterial species in the
494 stomach. Inflamm Res. 2010;59(12):997–1003.

495 6. Johnson KS, Ottemann KM. Colonization, localization, and inflammation: the roles of *H. pylori*
496 chemotaxis in vivo. Curr Opin Microbiol [Internet]. 2018;41:51–7.

497 7. Colin R, Sourjik V. Emergent properties of bacterial chemotaxis pathway. Curr Opin Microbiol
498 [Internet]. 2017;39:24–33.

499 8. Parkinson JS, Hazelbauer GL, Falke JJ. Signaling and sensory adaptation in Escherichia coli
500 chemoreceptors: 2015 update. Trends Microbiol [Internet]. 2015;23(5):257–66.

501 9. Porter SL, Wadhams GH, Armitage JP. Signal processing in complex chemotaxis pathways. Nat
502 Rev Microbiol [Internet]. 2011;9(3):153–65.

503 10. Wadhams GH, Armitage JP. Making sense of it all: Bacterial chemotaxis. Nat Rev Mol Cell Biol.
504 2004;5(12):1024–37.

505 11. Rolig AS, Shanks J, Carter JE, Ottemann KM. *Helicobacter pylori* requires TlpD-driven chemotaxis
506 to proliferate in the antrum. Infect Immun. 2012;80(10):3713–20.

507 12. Behrens W, Schweinitzer T, Bal J, Dorsch M, Bleich A, Kops F, et al. Role of energy sensor TlpD of

508 *Helicobacter pylori* in gerbil colonization and genome analyses after adaptation in the gerbil.
509 Infect Immun. 2013;81(10):3534–51.

510 13. Foynes S, Dorrell N, Ward SJ, Stabler RA, McColm AA, Rycroft AN, et al. *Helicobacter pylori*
511 possesses two CheY response regulators and a histidine kinase sensor, CheA, which are essential
512 for chemotaxis and colonization of the gastric mucosa. Infect Immun. 2000;68(4):2016–23.

513 14. Terry K, Williams SM, Connolly L, Ottemann KM. Chemotaxis plays multiple roles during
514 *Helicobacter pylori* animal infection. Infect Immun. 2005;73(2):803–11.

515 15. Alexander RP, Lowenthal AC, Harshey RM, Ottemann KM. CheV: CheW-like coupling proteins at
516 the core of the chemotaxis signaling network. Trends Microbiol. 2010;18(11):494–503.

517 16. Abedrabbo S, Castellon J, Collins KD, Johnson KS, Ottemann KM. Cooperation of two distinct
518 coupling proteins creates chemosensory network connections. Proc Natl Acad Sci U S A.
519 2017;114(11):2970–5.

520 17. Collins KD, Andermann TM, Draper J, Sanders L, Williams SM, Araghi C, et al. The *Helicobacter*
521 *pylori* CZB cytoplasmic chemoreceptor TlpD forms an autonomous polar chemotaxis signaling
522 complex that mediates a tactic response to oxidative stress. J Bacteriol. 2016;198(11):1563–75.

523 18. Pittman MS, Goodwin M, Kelly DJ. Chemotaxis in the human gastric pathogen *Helicobacter pylori:*
524 Different roles for CheW and the three CheV paralogues, and evidence for CheV2
525 phosphorylation. Microbiology. 2001;147(9):2493–504.

526 19. Ortega DR, Zhulin IB. Evolutionary Genomics Suggests That CheV Is an Additional Adaptor for
527 Accommodating Specific Chemoreceptors within the Chemotaxis Signaling Complex. PLoS
528 Comput Biol. 2016;12(2):1–19.

529 20. Jiménez-Pearson MA, Delany I, Scarlato V, Beier D. Phosphate flow in the chemotactic response
530 system of *Helicobacter pylori.* Microbiology. 2005;151(10):3299–311.

531 21. Lowenthal AC, Simon C, Fair AS, Mehmood K, Terry K, Anastasia S, et al. A fixed-time diffusion
532 analysis method determines that the three *cheV* genes of *Helicobacter pylori* differentially affect
533 motility. Microbiology. 2009;155(4):1181–91.

534 22. Collins KD, Lacal J, Ottemann KM. Internal Sense of Direction: Sensing and Signaling from
535 Cytoplasmic Chemoreceptors. Microbiol Mol Biol Rev [Internet]. 2014;78(4):672–84.

536 23. Draper J, Karplus K, Ottemann KM. Identification of a chemoreceptor zinc-binding domain
537 common to cytoplasmic bacterial chemoreceptors. J Bacteriol. 2011;193(17):4338–45.

538 24. Perkins A, Tudorica D, Amieva M. *Helicobacter pylori* Senses Bleach as a Chemoattractant Using a
539 Cytosolic Chemoreceptor. PLoS Biol. 2019;17(8):1–33.

540 25. Jumper J, Evans R, Pritzel A, Green T, Figurnov M, Ronneberger O, et al. Highly accurate protein
541 structure prediction with AlphaFold. Nature [Internet]. 2021;596(7873):583–9.

542 26. Kanehisa M, Goto S, Kawashima S, Nakaya A. The KEGG databases at GenomeNet. Nucleic Acids
543 Res. 2002;30(1):42–6.

544 27. Marchler-Bauer A, Bo Y, Han L, He J, Lanczycki CJ, Lu S, et al. CDD/SPARCLE: Functional
545 classification of proteins via subfamily domain architectures. Nucleic Acids Res.
546 2017;45(D1):D200–3.

547 28. Mooij WTM, Mitsiki E, Perrakis A. ProteinCCD: Enabling the design of protein truncation
548 constructs for expression and crystallization experiments. Nucleic Acids Res. 2009;37(SUPPL.
549 2):402–5.

550 29. Linding R, Russell RB, Neduva V, Gibson TJ. GlobPlot: Exploring protein sequences for globularity
551 and disorder. Nucleic Acids Res. 2003;31(13):3701–8.

552 30. Trivedi R, Nagarajaram HA. Intrinsically Disordered Proteins: An Overview. Int J Mol Sci.
553 2022;23(22):1–30.

554 31. Zähringer F, Lacanna E, Jenal U, Schirmer T, Boehm A. Structure and signaling mechanism of a
555 zinc-sensory diguanylate cyclase. Structure. 2013;21(7):1149–57.

556 32. Karimova G, Pidoux J, Ullmann A, Ladant D. A bacterial two-hybrid system based on a
557 reconstituted signal transduction pathway. Proc Natl Acad Sci U S A. 1998;95(10):5752–6.

558 33. Censini S, Lange C, Xiang Z, Crabtree JE, Ghiara P, Borodovsky M, et al. *cag*, a pathogenicity island
559 of *Helicobacter pylori*, encodes type I-specific and disease-associated virulence factors. Proc Natl
560 Acad Sci U S A. 1996;93(25):14648–53.

561 34. Williams SM, Chen YT, Andermann TM, Carter JE, McGee DJ, Ottemann KM. *Helicobacter pylori*
562 chemotaxis modulates inflammation and bacterium-gastric epithelium interactions in infected
563 mice. Infect Immun. 2007;75(8):3747–57.

564 35. Castillo AR, Arevalo SS, Woodruff AJ, Ottemann KM. Experimental analysis of *Helicobacter pylori*
565 transcriptional terminators suggests this microbe uses both intrinsic and factor-dependent
566 termination. Mol Microbiol. 2008;67(1):155–70.

567 36. Rader BA, Wreden C, Hicks KG, Sweeney EG, Ottemann KM, Guillemin K. *Helicobacter pylori*
568 perceives the quorum-sensing molecule AI-2 as a chemorepellent via the chemoreceptor TlpB.
569 Microbiology. 2011;157(9):2445–55.

570 37. Lertsethtakarn P, Howitt MR, Castellon J, Amieva MR, Ottemann KM. *Helicobacter pylori* CheZ
571 and ChePep form a novel chemotaxis-regulatory complex distinct from the core chemotaxis
572 signaling proteins and the flagellar motor. Mol Microbiol. 2015;97(6):1063–78.

573 38. Chandrashekhar K, Kassem II, Rajashekara G. *Campylobacter jejuni* transducer like proteins:
574 Chemotaxis and beyond. Gut Microbes. 2017;8(4):323–34.

575 39. Behrens W, Schweinitzer T, McMurry JL, Loewen PC, Buettner FFR, Menz S, et al. Localisation and
576 protein-protein interactions of the *Helicobacter pylori* taxis sensor TlpD and their connection to
577 metabolic functions. Sci Rep [Internet]. 2016;6(December 2015):1–20.

578 40. Rain J, Selig L, De Reuse H, Battaglia V, Reverdy C, Simon S, et al. The protein-protein interaction
579 map of *Helicobacter pylori*. Nature. 2001;409(6817):211–5.

580 41. Bennett HJ, Roberts IS. Identification of a new sialic acid-binding protein in *Helicobacter pylori.*
581 FEMS Immunol Med Microbiol. 2005;44(2):163–9.

582 42. Hauser R, Ceol A, Rajagopala S V., Mosca R, Siszler G, Wermke N, et al. A second-generation
583 protein-protein interaction network of *Helicobacter pylori*. Mol Cell Proteomics [Internet].
584 2014;13(5):1318–29.

585 43. Castellon J. CheV1 Leads the Organization of Chemotaxis Signal Transduction Proteins in
586 *Helicobacter pylori*. UC Santa Cruz [Internet]. 2013; Available from:
587 https://escholarship.org/uc/item/4sz47014

588 44. Bardy SL, Maddock JR. Polar localization of a soluble methyl-accepting protein of *Pseudomonas*
589 *aeruginosa.* J Bacteriol. 2005;187(22):7840–4.

590 45. Meier VM, Scharf BE. Cellular localization of predicted transmembrane and soluble
591 chemoreceptors in *Sinorhizobium meliloti*. J Bacteriol. 2009;191(18):5724–33.

592 46. Cannistraro VJ, Glekas GD, Rao C V., Ordal GW. Cellular stoichiometry of the chemotaxis proteins
593 in *Bacillus subtilis*. J Bacteriol. 2011;193(13):3220–7.

594 47. Xie Z, Ulrich LE, Zhulin IB, Alexandre G. PAS domain containing chemoreceptor couples dynamic
595 changes in metabolism with chemotaxis. Proc Natl Acad Sci U S A. 2010;107(5):2235–40.

596 48. Jones CW, Armitage JP. Positioning of bacterial chemoreceptors. Trends Microbiol [Internet].
597 2015;23(5):247–56.

598 49. Frye J, Karlinsey JE, Felise HR, Marzolf B, Dowidar N, McClelland M, et al. Identification of new
599 flagellar genes of *Salmonella enterica* serovar typhimurium. J Bacteriol. 2006;188(6):2233–43.

600 50. Schultz J, Milpetz F, Bork P, Ponting CP. SMART, a simple modular architecture research tool:
601 Identification of signaling domains. Proc Natl Acad Sci U S A. 1998;95(11):5857–64.

602 51. Wang Q, Mariconda S, Suzuki A, McClelland M, Harshey RM. Uncovering a large set of genes that
603 affect surface motility in *Salmonella enterica* serovar typhimurium. J Bacteriol.
604 2006;188(22):7981–4.

605 52. Lazova MD, Butler MT, Shimizu TS HR. Salmonella chemoreceptors McpB and McpC mediate a
606 repellent response to L-cystine: a potential mechanism to avoid oxidative conditions. Mol
607 Microbiol. 2012;84(4):697–711.

608 53. Hu S, Giacopazzi S, Modlin R, Karplus K, Bernick DL, Ottemann KM. Altering under-represented
609 DNA sequences elevates bacterial transformation efficiency. MBio. 2023;14(6):1–6.

610 54. Ottemann KM, Lowenthal AC. *Helicobacter pylori* uses motility for initial colonization and to
611 attain robust infection. Infect Immun. 2002;70(4):1984–90.

612 55. McGee DJ, Langford ML, Watson EL, Carter JE, Chen YT, Ottemann KM. Colonization and
613 inflammation deficiencies in Mongolian gerbils infected by *Helicobacter pylori* chemotaxis
614 mutants. Infect Immun. 2005;73(3):1820–7.

615 56. Lowenthal AC, Hill M, Sycuro LK, Mehmood K, Salama NR, Ottemann KM. Functional analysis of
616 the *Helicobacter pylori* flagellar switch proteins. J Bacteriol. 2009;191(23):7147–56.

617 57. Miller JH. Experiments in Molecular Genetics. Cold Spring Harbor Laboratory; 1972. 466 p.

618

619 **Supporting information**

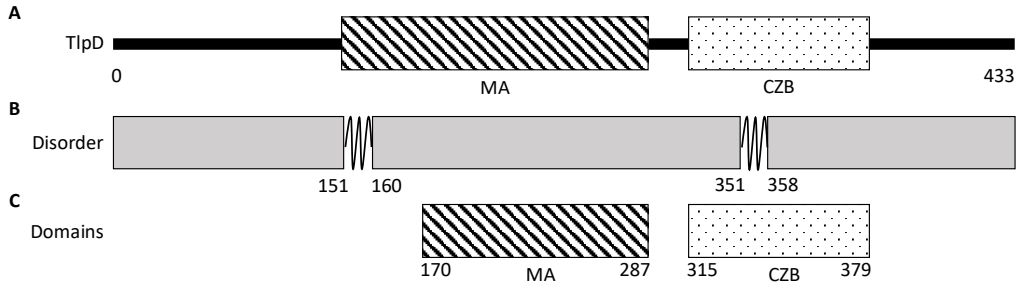

620

621 **S1 Fig. Summary of Predicted secondary structures and domains of TlpD.** (A) Full-length TlpD for

622 reference. (B) Predicted TlpD globular regions in grey and the unstructured regions shown as twists. (C)

623 Predicted TlpD domains with the two highest scores, the MA and CZB domain.

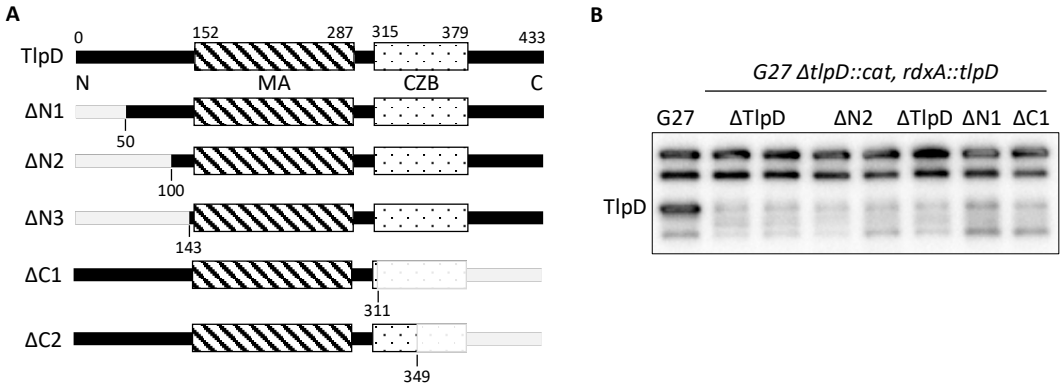

624

625 **S2 Fig. First generation of TlpD truncation constructs and expression in *H. pylori*.** (A) Modified versions

626 of *H. pylori* TlpD with domains and truncation sites (grey). TlpD is the full-length version of the protein at

627 433 amino acids, ΔTlpD are negative background controls, ΔN1 is truncated at residue 50, ΔN2 is

628 truncated at residue 100, ΔN3 is truncated at residue 143, ΔC1 is truncated at residue 311, and ΔC2 is

629 truncated at residue 349. (B) Western blot of *H. pylori* G27 strains with complemented *tlpD* constructs

630 were analyzed from whole-cell lysates with an anti-TlpA-22 antibody [34] which recognizes the

631 conserved MA domain of all chemoreceptors. The expected size of wild-type TlpD is 48 kDa, ΔN1 is 42.9

632 kDa, ΔN2 is 37.4 kDa, and ΔC1 is 34 kDa. Western blots are representative of 3 biological replicates.

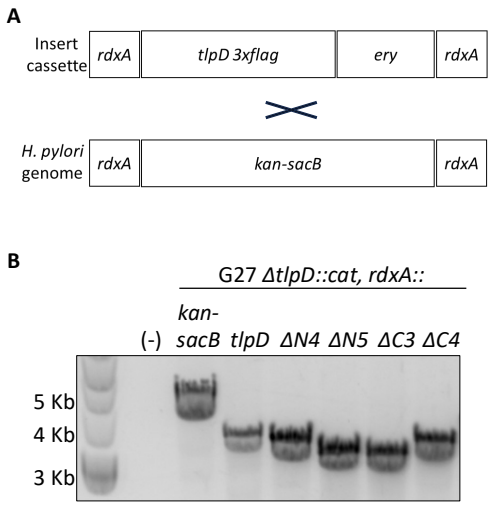

S3 Fig. *tlpD* sequence layout for transformation into the *H. pylori* genome. (A) Design of *tlpD* insert cassette for transformation into *H. pylori*. This cassette contains the *tlpD* sequence, a *3xflag* tag and *erythromycin* (*ery*) resistance sequences that are flanked by *rdxA* homologous regions for integration into the *H. pylori* genome at the *rdxA* locus. (B) PCR of erythromycin resistant *H. pylori* isolates using primers that flank the *rdxA* locus. The nomenclature above each band indicates the amplified product. (-); PCR no template control. *kan-sacB*; kanamycin resistance and sucrose sensitivity selection marker present in the *H. pylori* transformation background and serves as a negative control. *tlpD*, ΔN4, ΔN5, ΔC3, ΔC4 are the versions of *tlpD* on the cassette that were PCR amplified.

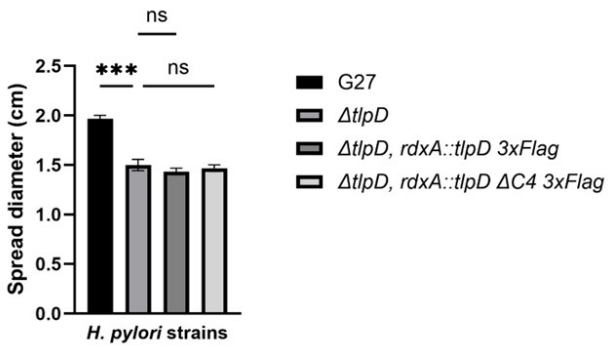

S4 Fig. *H. pylori* that express complemented TlpD in conjunction with chemoreceptors TlpA and TlpB phenocopy an isogenic *ΔtlpD* mutant on soft agar. G27 wild-type and mutants were analyzed for

645 chemotaxis by soft agar spreading. Strains were stabbed onto soft agar and spreading was tracked and
646 measured after 3 days. Strains included are a tlpD null version of G27 complemented with a full-length
647 tagged version of TlpD (*rdxA::tlpD 3xFlag*) or TlpDΔC4 (*rdxA::tlpD Δ4 3xFlag*). Wild-type G27 is a positive
648 control. G27 *ΔtlpD* is a chemoreceptor negative control. Spread diameter (cm) of G27 strains was
649 measured on day 5. Error bars indicate the SEMs. Strains were analyzed statistically by an ordinary one-
650 way ANOVA comparing the mean of each column with the mean of the *ΔtlpD* column. ***P<0.001.

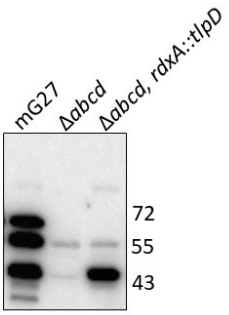

651

652 **S5 Fig. TlpD is produced when complemented into *H. pylori* that lacks all chemoreceptors.** Western
653 blot of *H. pylori* mG27 *Δabcd* expressing complemented WT *tlpD* was analyzed from whole-cell lysates
654 with an anti-TlpA22 antibody which recognizes the MA domain. The strains analyzed are indicated at the
655 top. Marker sizes are given in kilodaltons on the right. The expected size of TlpD is 48 kDa. Western blot
656 is representative of 2 biological replicates.

S3 Table. Primers used in this study.

Primer	Oligonucleotide sequence
rdxA Fwd	cgccattcttgcaagatgtttg
rdxA Rev	ctcgcttctgccaccctctt
tlpD pUT18 Fwd	agatCTGCAGatgtttgggaataagcagttac[a]
tlpD pUT18 Rev	ggagGGTACCttcgccttttttgaatttttttcaatg[a]
ΔC4 pUT18 Fwd	aattCTGCAGatgtttgggaataagcagttacagc[a]
ΔC4 pUT18 Rev	gagaGGTACCggtaatgtggtcttcttgaacg[a]

657 [a]Restriction sites are capitalized.

658 **S1 File. TlpD secondary structure bioinformatic analysis.**
659 **S2 File. *tlpD* plasmid sequences.**